



Publications

1997

Velocity–Space Drag and Diffusion in a Model, Two-Dimensional Plasma

Mark Anthony Reynolds
Embry-Riddle Aeronautical University, reynoldb2@erau.edu

B.D. Fried
University of California, Los Angeles

G.J. Morales
University of California, Los Angeles

Follow this and additional works at: <https://commons.erau.edu/publication>



Part of the [Plasma and Beam Physics Commons](#)

Scholarly Commons Citation

Reynolds, M. A., Fried, B., & Morales, G. (1997). Velocity–Space Drag and Diffusion in a Model, Two-Dimensional Plasma. *Physics of Plasmas*, 4(). Retrieved from <https://commons.erau.edu/publication/395>

This Article is brought to you for free and open access by Scholarly Commons. It has been accepted for inclusion in Publications by an authorized administrator of Scholarly Commons. For more information, please contact commons@erau.edu.

Velocity-space drag and diffusion in a model, two-dimensional plasma

M. A. Reynolds,^{a)} B. D. Fried, and G. J. Morales

Department of Physics and Astronomy, University of California, Los Angeles, California 90095

(Received 3 January 1997; accepted 14 February 1997)

The quasilinear fluctuation integral is calculated for a two-dimensional, unmagnetized plasma (composed of charged rods), and is expressed in terms of Fokker-Planck coefficients. It is found that in two dimensions, the enhanced fluctuations generated by fast electrons lead to anomalously large transport coefficients. In particular, the effect of a small population of fast electrons is only weakly dependent on their density. In three dimensions, the effect of fast electrons is masked by the dominant approximation, but higher-order terms describe processes similar to those in two dimensions, and these terms can become significant for weakly stable plasmas. The differences between two and three dimensions arise from the fact that both emission and damping of plasma waves are retained to lowest order in two dimensions, while the three-dimensional dominant approximation effectively includes only wave emission by test particles. An understanding of the differences between two and three dimensions is crucial to the interpretation of two-dimensional particle simulations. © 1997 American Institute of Physics. [S1070-664X(97)03605-7]

I. INTRODUCTION

There has recently been renewed interest in plasma-wave energy transport, as well as the related topic of fluctuations due to fast electrons. Ware¹ derived a Fokker-Planck equation to describe the time evolution of fast electrons due to wave emission and absorption in a strongly magnetized plasma. This result, which ignores the Coulomb logarithm term of the dominant approximation² and focuses on the higher-order wave terms (which become appreciable for fast electrons), is identical in character to the Fokker-Planck coefficients due to enhanced fluctuations in an unmagnetized plasma derived by Tidman and Eviatar.³

The present investigation centers on a calculation of the Fokker-Planck coefficients for a two-dimensional, isotropic plasma with a low-density component of fast electrons. This scenario sheds light on the role of emission and damping of electrostatic waves in the relaxation of weakly stable plasmas. Two dimensions provide a convenient paradigm because, unlike three dimensions, the transport due to waves dominates collisional effects. No dominant approximation is needed since the Coulomb potential in two dimensions is logarithmic, and because wave effects are prevalent, there is an enhanced interaction between fast electrons. That is, a fast test electron experiences anomalously large drag and diffusion forces due to the enhanced fluctuations generated by a low-density, fast-electron population. Of course, fast electrons also generate enhanced fluctuations in three dimensions,^{1,3} but for plasmas near equilibrium, their effect on transport is largely masked by collisional processes.^{4,5}

Similar work related to two-dimensional particle simulations was carried out by Okuda and Birdsall⁶ and Langdon and Birdsall.⁷ They were primarily interested in the effects that the finite size of the particles had on collisions (in both two and three dimensions) and in the unphysical k spectrum generated by the spatial grid. In fact, one of their primary

motivations was to show that the high collision rates associated with low-density plasma simulations could be lowered when the finite particle size was included. This allowed simulations with a reasonable number of particles to give meaningful results. The present work, however, is concerned with the intrinsic properties of two-dimensional relaxation processes, i.e., the relaxation of two-dimensional, point particles, and the anomalous effects that appear in two dimensions.

Computer simulations do show that wave emission and damping are important mechanisms in relaxation processes. Decyk *et al.*⁸ initialized a two-and-a-half-dimensional particle-in-cell simulation with a “slideaway” electron tail in a narrow, field-aligned region, and investigated the relaxation. Three of their results are relevant to the present study. The most important finding is that the distribution of fast electrons relaxes approximately ten times more rapidly than the total electron current. That is, the electron distribution function redistributes itself into two half-Maxwellians with different temperatures (hence with a net drift), and only exchanges momentum with the ions more slowly. This suggests that something other than classical collisional processes are responsible. Second, the frequency spectrum of the electric field is enhanced over the range of frequencies that satisfies $\omega = k_{\parallel}v$, where v is the velocity of the particles in the tail. This points explicitly to the fast electrons as wave exciters. A third finding is the significant spatial diffusion of current across the magnetic field, even though the particles themselves are restricted from crossing field lines and the electron cyclotron radius is small. These results imply that wave activity, rather than collisions, is responsible for the velocity relaxation and current transport in this environment.

This paper is organized as follows. In Sec. II we describe the differences between two and three dimensions, and how the predominance of wave effects in two dimensions results from the form of the Coulomb potential. The two-dimensional fluctuation integral, derived in the Appendix, is evaluated in Sec. III for various velocity distributions. The enhanced interaction between fast electrons, due to the inher-

^{a)}Present address: Beam Physics Branch, Plasma Physics Division, Naval Research Laboratory, Washington, D.C. 20375.

ent inclusion of both wave emission and wave damping, is examined in detail, and it is found that the Fokker–Planck coefficients for a test electron due to a tail population of fast electrons is very weakly dependent on the density of that population. In Sec. IV we compare the two-dimensional results with the higher-order effects in three dimensions. In Sec. V we evaluate the two-dimensional frequency spectrum derived in the Appendix and show an enhancement above the plasma frequency due to the fast electrons. Conclusions are presented in Sec. VI.

II. TWO-DIMENSIONAL CHARACTER

There are two major approaches to the calculation of the Fokker–Planck coefficients. The collisional approach makes the same assumption as the kinetic theory of neutral gases, namely that only binary interactions cause changes in the distribution function, while the fluctuational approach emphasizes the role of collective interactions. Each approach has complementary domains of validity (small distances and large distances, respectively), and the two domains do not necessarily overlap, but in three dimensions the two methods give similar results. In two dimensions, however, the concept of binary collisions is of limited usefulness.

When evaluating the collision integral in three dimensions, the $1/r$ potential necessitates a cutoff.^{9–11} In two dimensions, the range of the $\ln r$ potential is even longer. But, even though the number of interacting particles increases only as r^2 (rather than r^3), the long range makes an analytic treatment of collisions impossible.¹² This is because the collision approach requires a calculation of the differential cross section, which in turn requires a knowledge of the impact parameter as a function of the deflection angle. For oppositely charged particles, there are no unbound orbits in two dimensions, which means that the cross section is not defined. The only possible solution is to eliminate the long range feature of the potential by using the Debye-shielded potential, and calculate the collisional dynamics numerically. This approximation is neither easy nor useful. (A further approximation, the impulse approximation, reveals that the collision integral does not diverge at a large impact parameter so that the use of the impulse approximation is inconsistent.¹²) However, using the Debye-shielded potential is equivalent to taking the limit of static shielding in the fluctuational approach.

The fluctuational approach incorporates the long-distance, Debye-shielded behavior correctly, but the small-distance behavior diverges. In three dimensions, the core of the $1/r$ potential is too “hard,” so the divergent integral must also be cut off. The core of $\ln r$ is softer, and no cutoff is needed: the integrals may be evaluated exactly. However, cutting off integrals in three dimensions results in the Coulomb logarithm, which lumps all kinetic information into one factor. The convergent behavior of the two-dimensional integral thus includes kinetic information of the background plasma. Specifically, characteristics of the dispersion relation play a crucial role in determining transport properties. When the plasma is in thermodynamic equilibrium, the extra kinetic information does not significantly affect the behavior of the transport coefficients, and two dimensions is similar to

the three-dimensional dominant approximation. However, when nonthermal distributions are considered, especially fast electrons, anomalous properties appear in two dimensions that have no counterpart in the dominant approximation of three dimensions, but are similar to the higher-order terms.^{1,3} Decker *et al.*¹³ reached a similar conclusion when they showed that the zero-frequency limit of the electron–ion collision frequency is proportional to the well-known $\ln \Lambda/n\lambda_D^3$ in three dimensions (where $\Lambda = n\lambda_D^3$, the number of particles in a Debye cube), but only $1/n\lambda_D^2$ in two dimensions. The predominance of waves eliminates the need for the dominant approximation and hence the $\ln \Lambda$.

III. TRANSPORT COEFFICIENTS DUE TO FLUCTUATIONS

The Fokker–Planck equation can be written in the form

$$\frac{\delta f}{\delta t} = -\frac{\partial}{\partial \mathbf{v}} \cdot (\mathbf{A}f) + \frac{1}{2} \frac{\partial}{\partial \mathbf{v}} \cdot \left(\mathbf{D} \cdot \frac{\partial f}{\partial \mathbf{v}} \right), \quad (1)$$

where $f(\mathbf{v})$ is the velocity distribution, $\delta f/\delta t$ represents the non-Vlasov change in f , and $\mathbf{A}(\mathbf{v})$ and $\mathbf{D}(\mathbf{v})$ are the drag and diffusion coefficients, respectively. The fluctuation integral of Lenard¹⁴ is rederived in the Appendix for application to fewer than three dimensions by considering a quasilinear extension of the Vlasov equation. An identical result can be obtained from a Fokker–Planck calculation, where the fluctuating field (rather than binary collisions) gives rise to changes in velocity. It is found that the form of $\delta f/\delta t$, aside from a numerical factor that simply counts the number of spatial Fourier transforms, is independent of the spatial dimension. For particles of mass m and charge q the result is [see Eqs. (A5)]

$$\frac{\delta f}{\delta t} = -\frac{\partial}{\partial \mathbf{v}} \cdot \mathbf{J}(\mathbf{v}), \quad (2a)$$

$$\mathbf{J}(\mathbf{v}) = \frac{1}{(2\pi)^{\nu-3}} \sum_{\sigma} \int d^{\nu} v_{\sigma} \left(\frac{f(\mathbf{v})}{m_{\sigma}} \frac{\partial f_{\sigma}(\mathbf{v}_{\sigma})}{\partial \mathbf{v}_{\sigma}} - \frac{f_{\sigma}(\mathbf{v}_{\sigma})}{m} \frac{\partial f(\mathbf{v})}{\partial \mathbf{v}} \right) \cdot \mathbf{K}, \quad (2b)$$

$$\mathbf{K} = \frac{2q^2 q_{\sigma}^2 n_{\sigma}}{m} \int d^{\nu} k \frac{\delta(\mathbf{k} \cdot \mathbf{v} - \mathbf{k} \cdot \mathbf{v}_{\sigma})}{|\epsilon(\mathbf{k}, \mathbf{k} \cdot \mathbf{v})|^2} \frac{\mathbf{k} \mathbf{k}}{k^4}, \quad (2c)$$

where ν is the spatial dimension (1, 2, or 3), \sum_{σ} is a sum over all species σ , and ϵ is the dielectric function. In Eqs. (2) and the rest of this paper, symbols such as m , q , and n depend on the spatial dimension ν . For example, m is the mass of a particle in three dimensions, but is the mass *per unit length* of a particle in two dimensions. Equations (2) are seen to have the Fokker–Planck form, where the coefficients are

$$\mathbf{A}(\mathbf{v}) = \sum_{\sigma} \frac{2q^2 q_{\sigma}^2 n_{\sigma}}{m m_{\sigma} (2\pi)^{\nu-3}} \times \int d^{\nu} k d^{\nu} v_{\sigma} \frac{\delta(\mathbf{k} \cdot \mathbf{v} - \mathbf{k} \cdot \mathbf{v}_{\sigma})}{k^4 |\epsilon(\mathbf{k}, \mathbf{k} \cdot \mathbf{v})|^2} \mathbf{k} \mathbf{k} \cdot \frac{\partial f_{\sigma}(\mathbf{v}_{\sigma})}{\partial \mathbf{v}_{\sigma}}, \quad (3a)$$

$$\mathbf{D}(\mathbf{v}) = \sum_{\sigma} \frac{4q^2 q_{\sigma}^2 n_{\sigma}}{m^2 (2\pi)^{\nu-3}} \times \int d^{\nu} k d^{\nu} v_{\sigma} \frac{\delta(\mathbf{k} \cdot \mathbf{v} - \mathbf{k} \cdot \mathbf{v}_{\sigma})}{k^4 |\epsilon(\mathbf{k}, \mathbf{k} \cdot \mathbf{v})|^2} \mathbf{k} \mathbf{k} f_{\sigma}(\mathbf{v}_{\sigma}). \quad (3b)$$

To consider \mathbf{A} and \mathbf{D} in more detail, the distribution function first is assumed isotropic so that the velocity integrations are trivial. This reveals why the dominant approximation is needed in three dimensions but not in two. Second, Maxwellian distributions are used to evaluate \mathbf{A} and \mathbf{D} explicitly.

A. Isotropic distributions

When the distribution functions are isotropic, the velocity integrations are trivial because the δ function takes care of the component of \mathbf{v} parallel to \mathbf{k} , and the integrations over the components of \mathbf{v} transverse to \mathbf{k} are given by the normalization (which has been defined as $\int d^{\nu} v f = 1$). The velocity integrations become

$$\int d^{\nu} v_{\sigma} f_{\sigma}(v_{\sigma}) \delta(\mathbf{k} \cdot \mathbf{v} - \mathbf{k} \cdot \mathbf{v}_{\sigma}) = \frac{f_{\sigma}^1(\hat{\mathbf{k}} \cdot \mathbf{v})}{k}, \quad (4a)$$

$$\int d^{\nu} v_{\sigma} \mathbf{k} \cdot \frac{\partial f_{\sigma}(v_{\sigma})}{\partial \mathbf{v}_{\sigma}} \delta(\mathbf{k} \cdot \mathbf{v} - \mathbf{k} \cdot \mathbf{v}_{\sigma}) = \frac{\partial f_{\sigma}^1(\hat{\mathbf{k}} \cdot \mathbf{v})}{\partial(\hat{\mathbf{k}} \cdot \mathbf{v})}, \quad (4b)$$

where f_{σ}^1 is defined as the one-dimensional distribution function for species σ after integrating over the velocities perpendicular to \mathbf{k} ,

$$f^1(v_{\parallel}) \equiv \int d^{\nu-1} v_{\perp} f(v). \quad (5)$$

For isotropic distributions the dielectric function can be written as

$$\epsilon(\mathbf{k}, \omega) = 1 - \sum_{\sigma} \frac{\omega_{p\sigma}^2}{2k^2 \bar{v}_{\sigma}^2} \mathcal{Z}'\left(\frac{\omega}{\sqrt{2}k\bar{v}_{\sigma}}\right), \quad (6)$$

where \mathcal{Z} is a generalized plasma dispersion function and is defined as

$$\mathcal{Z}' \equiv 2\bar{v}_{\sigma}^2 \int d^{\nu} v \frac{\mathbf{k} \cdot \hat{\mathbf{v}}}{\mathbf{k} \cdot \mathbf{v} - \omega} \frac{\partial f_{\sigma}(v)}{\partial v}. \quad (7)$$

Of course, when the distribution function is Maxwellian, \mathcal{Z} becomes Z , the well-known plasma dispersion function.¹⁵ To evaluate Eqs. (3), the quantity $\epsilon(\mathbf{k}, \mathbf{k} \cdot \mathbf{v})$ is also needed. It can be written in terms of ξ , a complex function of $\hat{\mathbf{k}} \cdot \mathbf{v} = v \cos \theta$ (but independent of k),

$$\epsilon(\mathbf{k}, \mathbf{k} \cdot \mathbf{v}) = 1 - \xi^2/k^2, \quad (8)$$

$$\xi^2 \equiv \sum_{\sigma} \frac{\omega_{p\sigma}^2}{2\bar{v}_{\sigma}^2} \mathcal{Z}'\left(\frac{v \cos \theta}{\sqrt{2}\bar{v}_{\sigma}}\right). \quad (9)$$

With the definitions in Eqs. (5) and (9), the general form of \mathbf{A} and \mathbf{D} for arbitrary isotropic distributions are

$$\mathbf{A}(\mathbf{v}) = \sum_{\sigma} \frac{2q^2 q_{\sigma}^2 n_{\sigma}}{mm_{\sigma} (2\pi)^{\nu-3}} \times \int d^{\nu} k \frac{\mathbf{k}}{|k^2 - \xi^2|^2} \frac{\partial f_{\sigma}^1(v \cos \theta)}{\partial(v \cos \theta)}, \quad (10)$$

$$\mathbf{D}(\mathbf{v}) = \sum_{\sigma} \frac{4q^2 q_{\sigma}^2 n_{\sigma}}{m^2 (2\pi)^{\nu-3}} \int d^{\nu} k \frac{\mathbf{k} \mathbf{k}}{|k^2 - \xi^2|^2} f_{\sigma}^1(v \cos \theta). \quad (11)$$

The final step in obtaining the standard form is to make use of the fact that in an isotropic medium \mathbf{D} must have the form

$$\mathbf{D}(\mathbf{v}) = D_{\parallel}(v) \hat{\mathbf{v}} \hat{\mathbf{v}} + D_{\perp}(v) (\mathbf{I} - \hat{\mathbf{v}} \hat{\mathbf{v}}). \quad (12)$$

The parallel component has the same form in all dimensions,

$$D_{\parallel}(v) = \mathbf{D}(\mathbf{v}) : \hat{\mathbf{v}} \hat{\mathbf{v}}, \quad (13)$$

while the perpendicular component depends on ν (due to the fact that $\text{Tr } \mathbf{I} = \nu$),

$$D_{\perp}(v) = \frac{\text{Tr } \mathbf{D}(\mathbf{v}) - D_{\parallel}(v)}{\nu - 1}. \quad (14)$$

Perpendicular diffusion cannot occur in one dimension; correspondingly, D_{\perp} is undefined when $\nu = 1$. Vectors, such as \mathbf{A} , can be written in the form

$$\mathbf{A}(\mathbf{v}) = A_{\parallel}(v) \hat{\mathbf{v}} + \mathbf{A}_{\perp}(\mathbf{v}), \quad (15)$$

but the only nonzero component of \mathbf{A} is in the parallel direction,

$$A_{\parallel}(v) = \mathbf{A}(\mathbf{v}) \cdot \hat{\mathbf{v}}. \quad (16)$$

The perpendicular component of \mathbf{A} is proportional to $\mathbf{v} \times \hat{\mathbf{k}} = v \sin \theta$, so the integral over \mathbf{k} vanishes. Using the relations $\text{Tr } \mathbf{k} \mathbf{k} = k^2$ and $d^{\nu} k = d\Omega_{\nu} dk k^{\nu-1}$ (where $d\Omega_{\nu}$ is the differential solid angle in ν dimensions), the parallel and perpendicular components of \mathbf{A} and \mathbf{D} can be written in the standard form as a sum over species,

$$\begin{aligned} A_{\parallel} &= \sum_{\sigma} A_{\parallel}^{\sigma} \\ &= \sum_{\sigma} \frac{2q^2 q_{\sigma}^2 n_{\sigma}}{mm_{\sigma} (2\pi)^{\nu-3}} \int d\Omega_{\nu} \cos \theta \frac{\partial f_{\sigma}^1(v \cos \theta)}{\partial(v \cos \theta)} \\ &\quad \times \int dk \frac{k^{\nu}}{|k^2 - \xi^2|^2}, \end{aligned} \quad (17a)$$

$$\begin{aligned} D_{\parallel} &= \sum_{\sigma} D_{\parallel}^{\sigma} \\ &= \sum_{\sigma} \frac{4q^2 q_{\sigma}^2 n_{\sigma}}{m^2 (2\pi)^{\nu-3}} \int d\Omega_{\nu} \cos^2 \theta f_{\sigma}^1(v \cos \theta) \\ &\quad \times \int dk \frac{k^{\nu}}{|k^2 - \xi^2|^2}, \end{aligned} \quad (17b)$$

$$\begin{aligned}
D_{\perp} &= \sum_{\sigma} D_{\perp}^{\sigma} \\
&= \sum_{\sigma} \frac{4q^2 q_{\sigma}^2 n_{\sigma}}{m^2 (2\pi)^{\nu-3} (\nu-1)} \int d\Omega_{\nu} \sin^2 \theta f_{\sigma}^1(v \cos \theta) \\
&\quad \times \int dk \frac{k^{\nu}}{|k^2 - \xi^2|^2}. \tag{17c}
\end{aligned}$$

These coefficients, A_{\parallel}^{σ} , D_{\parallel}^{σ} , and D_{\perp}^{σ} , represent the drag and diffusion experienced by a test particle of mass m , charge q , and velocity v , due to species σ . All of the integrals over dk in Eqs. (17) are identical,

$$\mathcal{T}_{\nu}(\xi) \equiv \int dk \frac{k^{\nu}}{|k^2 - \xi^2|^2}, \tag{18}$$

and lead explicitly to the dominant approximation in three dimensions and an enhanced fast electron interaction in two dimensions.

In three dimensions \mathcal{T}_3 diverges logarithmically: for plasmas near equilibrium the upper limit of integration is approximated by k_m , the inverse of the distance of closest approach, and only the largest term is retained (the dominant approximation). This results in the usual Coulomb logarithm,

$$\mathcal{T}_3 \approx \ln \frac{k_m}{k_D} \equiv \ln \Lambda, \tag{19}$$

and is a physically acceptable solution because collective effects do not apply at small distances. However, while giving a finite answer, this technique throws away the kinetic information contained in ξ that is included in higher-order terms. Tidman and Eviatar³ showed that for weakly stable three-dimensional plasmas the higher-order terms can be approximated as

$$\mathcal{T}_3 \approx \ln \Lambda + \frac{\pi}{2} \frac{\text{Re } \xi}{|\text{Im } \xi|}. \tag{20}$$

Discussion of this result is deferred until Sec. IV.

In two dimensions, because of the soft core of the Coulomb potential, \mathcal{T}_2 retains information about the distribution function and the dispersion relation through ξ ,

$$\mathcal{T}_2 = -\frac{\pi}{4 \text{Im } \xi}. \tag{21}$$

This result was first obtained by Abraham-Shrauner¹⁶ who compared the two-dimensional Lenard-Balescu equation with the Landau equation for a Lorentzian velocity distribution and found significant differences. The disparity at large velocity between the two approaches was found to be larger than in three dimensions, but this was partly due to the non-physical distribution used. The coefficients are evaluated in Sec. III B for the more realistic Maxwellian distribution with fast electrons and the results are related to wave-driven transport.

In one dimension (i.e., a plasma of charged sheets), kinetic information is also retained but results in unphysical behavior. For example, stable (but nonequilibrium) distributions do not relax toward equilibrium distributions. The

properties of one-dimensional plasmas were investigated by Dawson^{17,18} and Eldridge and Feix^{19,20} in the 1960s, and have also recently been reexamined.²¹

B. Maxwellian distributions

A further simplification occurs when the distribution function of each species is a normalized Maxwellian,

$$f_{\sigma}(v) = \frac{e^{-u_{\sigma}^2}}{(\sqrt{2\pi\bar{v}_{\sigma}})^{\nu}}, \tag{22}$$

where $u_{\sigma} = v/\sqrt{2\bar{v}_{\sigma}}$. The one-dimensional distribution function f_{σ}^1 and its derivative are independent of ν ,

$$f_{\sigma}^1(v) = \frac{e^{-u_{\sigma}^2}}{\sqrt{2\pi\bar{v}_{\sigma}}}, \tag{23}$$

$$\frac{\partial f_{\sigma}^1(v)}{\partial v} = -\frac{v e^{-u_{\sigma}^2}}{\sqrt{2\pi\bar{v}_{\sigma}}^3}. \tag{24}$$

Also, $\mathcal{L} \rightarrow \mathcal{Z}$, which means that

$$\xi^2 \rightarrow \xi_M^2 = \sum_{\alpha} \frac{\omega_{p\sigma}^2}{2\bar{v}_{\sigma}^3} \mathcal{Z}'(u_{\sigma} \cos \theta). \tag{25}$$

In three dimensions, when the dominant approximation is used, the angular integrations can be expressed in terms of the error function, and are proportional to $\ln \Lambda$.²² Because of this simple proportionality, the coefficients due to each species (A_{\parallel}^{σ} , D_{\parallel}^{σ} , and D_{\perp}^{σ}) are self-similar: their dependence on velocity is only through u_{σ} . The full coefficients (A_{\parallel} , D_{\parallel} , and D_{\perp}) can be obtained by a simple scaling. There are four properties of the three-dimensional coefficients that warrant discussion. First, all the coefficients fall off with large velocity, as expected, because the interaction time with any given particle decreases with velocity. The asymptotic dependences on velocity are

$$A_{\parallel}^{\sigma} \sim 1/u_{\sigma}^2, \tag{26a}$$

$$D_{\parallel}^{\sigma} \sim 1/u_{\sigma}^3, \tag{26b}$$

$$D_{\perp}^{\sigma} \sim 1/u_{\sigma}, \tag{26c}$$

which shows that pitch-angle scattering dominates for large velocities (i.e., D_{\perp} falls off the slowest). Second, there is no drag when $v \approx 0$, but there is diffusion: particles may experience a random walk, but of course feel no frictional drag. Third, at intermediate velocities, the only structure occurs when $v \approx \bar{v}_{\sigma}$. That is, there is no indication that there are other species present. This is a consequence of the fact that only the emission of waves by the test particle is included in the dominant approximation—the damping due to other species is of higher order. Fourth, all the coefficients are proportional to the species density n_{σ} . This makes sense physically because the interaction with a group of particles is expected to be proportional to the quantity of those particles. The first two of these properties also hold true in two dimensions, because they are consequences of basic physical notions of interaction time and conservation of momentum. The last two, however, are only valid within the dominant ap-

proximation, and arise because the kinetic information, which contains the damping of the emitted waves, is neglected.

In two dimensions, the angular integrations are not expressible in terms of elementary functions because of the presence of $\text{Im } \xi$. They are, however, amenable to numerical computation. Because the results are not self-similar, the contributions of each species are investigated rather than the full coefficients. For simplicity, and in order to properly include the density dependence, the dimensionless equivalents of Eqs. (17), scaled to the corresponding electron quantities, are displayed. These are defined as

$$A_{\parallel} = -\frac{2q^2}{\sqrt{\pi m}(2\pi)^{\nu-3}} \left(\frac{q_e^2 n_e}{m_e \bar{v}_e^2 k_{De}} \right) \sum_{\sigma} \bar{A}_{\parallel}^{\sigma}, \quad (27a)$$

$$D_{\parallel} = \frac{4q^2}{\sqrt{2\pi m^2}(2\pi)^{\nu-3}} \left(\frac{q_e^2 n_e}{\bar{v}_e k_{De}} \right) \sum_{\sigma} \bar{D}_{\parallel}^{\sigma}, \quad (27b)$$

$$D_{\perp} = \frac{4q^2}{\sqrt{2\pi m^2}(2\pi)^{\nu-3}(\nu-1)} \left(\frac{q_e^2 n_e}{\bar{v}_e k_{De}} \right) \sum_{\sigma} \bar{D}_{\perp}^{\sigma}, \quad (27c)$$

where $k_{De} = w_{pe}/\bar{v}_e$,

$$\bar{A}_{\parallel}^{\sigma} \equiv k_{De} \left(\frac{q_{\sigma}^2 n_{\sigma}}{m_{\sigma} \bar{v}_{\sigma}^2} \right) \left(\frac{m_e \bar{v}_e^2}{q_e^2 n_e} \right) u_{\sigma} C_2^{\sigma}, \quad (28a)$$

$$\bar{D}_{\parallel}^{\sigma} \equiv k_{De} \left(\frac{q_{\sigma}^2 n_{\sigma}}{\bar{v}_{\sigma}} \right) \left(\frac{\bar{v}_e}{q_e^2 n_e} \right) C_2^{\sigma}, \quad (28b)$$

$$\bar{D}_{\perp}^{\sigma} \equiv k_{De} \left(\frac{q_{\sigma}^2 n_{\sigma}}{\bar{v}_{\sigma}} \right) \left(\frac{\bar{v}_e}{q_e^2 n_e} \right) S_2^{\sigma}, \quad (28c)$$

and in two dimensions the angular integrations are

$$C_2^{\sigma} \equiv -\frac{\pi}{4} \int_0^{2\pi} d\theta \frac{\cos^2 \theta e^{-u_{\sigma}^2 \cos^2 \theta}}{\text{Im } \xi_M(\theta)}, \quad (29a)$$

$$S_2^{\sigma} \equiv -\frac{\pi}{4} \int_0^{2\pi} d\theta \frac{\sin^2 \theta e^{-u_{\sigma}^2 \cos^2 \theta}}{\text{Im } \xi_M(\theta)}. \quad (29b)$$

In Eqs. (28) the factor k_{De} appears because ξ has units of inverse length.

To investigate the implications of two dimensions, a two-species plasma (electrons and singly charged ions) in thermal equilibrium ($n_e = n_i$ and $T_e = T_i$) and an ion-to-electron mass ratio of 64 is considered first. This mass ratio is chosen small in order to emphasize the effect of the ions, and also because particle simulations often use this value. Figure 1 shows \bar{A}_{\parallel}^i , \bar{D}_{\parallel}^i , and \bar{D}_{\perp}^i as functions of the scaled velocity u_e for such a plasma, while Fig. 2 shows the corresponding electron quantities. For this equilibrium situation there are interesting effects not present in three dimensions. Figure 1 reveals that the ion interaction is substantially unchanged in comparison with three dimensions (see Ref. 22). The only substantial difference from three dimensions is that the peak height of A_{\parallel} (and the widths of D_{\parallel} and D_{\perp}) occur near $v \approx 2\sqrt{2}\bar{v}$, rather than at $\sqrt{2}\bar{v}$ ($\sqrt{2}\bar{v}_i = 0.125$ on the scale of Fig. 1). Okuda and Birdsall⁶ found that this width in-

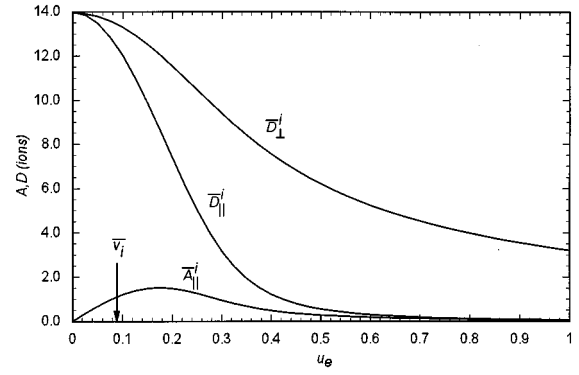


FIG. 1. Contribution of the ions to the Fokker-Planck coefficients of a test electron in a two-dimensional plasma in thermal equilibrium. The ion-to-electron mass ratio is 64.

creased with the size of the particles, but only calculated the coefficients for a single-species Maxwellian plasma, and hence did not illustrate the complex multispecies behavior. Figure 2 reveals a more complicated velocity dependence for the electron interaction. In addition to the $2\sqrt{2}\bar{v}$ width, all of the coefficients show structure between the ion thermal velocity \bar{v}_i and the electron thermal velocity \bar{v}_e , even though they represent an interaction with the electrons. The explanation of these effects requires a detailed consideration of Eqs. (29) in specific velocity regimes, which includes careful approximations to ξ_M .

1. Small velocities

The regime most similar to three dimensions is that of small velocities: $v \ll \bar{v}_i, \bar{v}_e$, or $u_e \ll u_i \ll 1$. In this case, the numerators of both C and S as well as the Z' function in ξ_M can be expanded for small u_{σ} ,

$$\xi_M^2 \approx -\sum_{\sigma} \frac{\omega_{p\sigma}^2}{\bar{v}_{\sigma}^2}, \quad (30)$$

$$= -k_D^2, \quad (31)$$

so that $\text{Im } \xi_M = -k_D$. The sign of the square root is chosen so that $\text{Im } \xi < 0$ (for reasons of causality). Because ξ_M is no

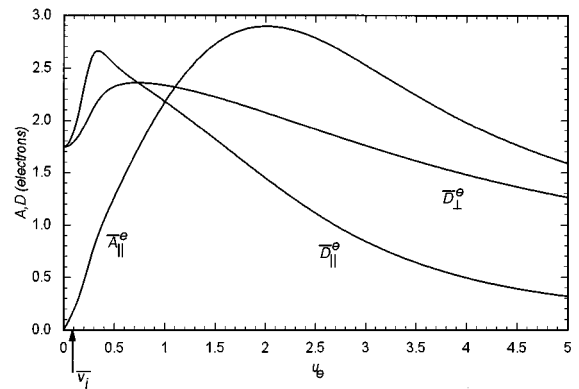


FIG. 2. Contribution of the electrons to the Fokker-Planck coefficients of a test electron in a two-dimensional plasma in thermal equilibrium. The ion-to-electron mass ratio is 64.

longer a function of θ , the angular integrations are straightforward, and to lowest order in u_σ they are constant,

$$C_2^\sigma \approx S_2^\sigma \approx \frac{\pi^2}{4k_D}. \quad (32)$$

Except for missing a factor of $\ln \Lambda$, this behavior is identical to that in three dimensions, including the fact that $D_\perp(0) = D_\parallel(0)$. This correspondence is expected because at small velocities the shielding of a test particle is static; the dynamical corrections are small.

At small velocities, then, particles do not experience the soft core of the logarithmic potential during collisions, and the exponential decay of the Debye-shielded potential is sufficiently similar to three dimensions that the drag and diffusion coefficients behave comparably.

2. Large velocities

In this regime, v is larger than both thermal velocities: $v \gg \bar{v}_i, \bar{v}_e$, or $1 \ll u_e \ll u_i$. Because the integrands of Eqs. (29) are sharply peaked, the usual asymptotic evaluation consists of approximating $(\text{Im } \xi_M)^{-1}$ as a constant over the region of integration,

$$C_2^\sigma \approx -\frac{\pi}{\text{Im } \xi_M(\theta_c)} \int_0^{\pi/2} d\theta \cos^2 \theta e^{-u_\sigma^2 \cos^2 \theta}, \quad (33a)$$

$$S_2^\sigma \approx -\frac{\pi}{\text{Im } \xi_M(\theta_s)} \int_0^{\pi/2} d\theta \sin^2 \theta e^{-u_\sigma^2 \cos^2 \theta}, \quad (33b)$$

where $\cos \theta_c = 1/u_\sigma$ and $\cos \theta_s = 0$. Strictly speaking, because the Z' function in ξ_M has the same argument as the exponential, and because its value varies substantially over the width of the exponential, the integrand of Eq. (29b) is not very sharply peaked. However, Eq. (33b) is the zeroth-order approximation to S_2^σ , and is adequate except for describing the enhanced tail interaction in Sec. III C. The remaining integrals can be evaluated in terms of Kummer confluent hypergeometric functions, which in the large-velocity approximation reduce to powers of u_σ ,

$$C_2^\sigma \approx -\frac{\pi \sqrt{\pi}}{4u_\sigma^3 \text{Im } \xi_M(\theta_c)}, \quad (34a)$$

$$S_2^\sigma \approx -\frac{\pi \sqrt{\pi}}{2u_\sigma \text{Im } \xi_M(\theta_s)}. \quad (34b)$$

As in the small-velocity regime, $\text{Im } \xi_M(\theta_s) = -k_D$, but the value of $\text{Im } \xi_M(\theta_c)$ depends on σ . That is, when $\sigma = e$, the electron term in the sum of Eq. (25) dominates and

$$\xi_M^2(\theta_c) \approx \frac{k_D^2}{4} Z'(1), \quad (35)$$

where $Z'(1) \approx 0.15 - 1.3i$, so that $\text{Im } \xi_M(\theta_c) \approx -0.38k_D$. On the other hand, when $\sigma = i$, both terms are comparable,

$$\xi_M^2(\theta_c) \approx \frac{k_D^2}{4} [Z'(1) - 2], \quad (36)$$

which gives $\text{Im } \xi_M(\theta_c) \approx -0.72k_D$. The final results are

$$C_2^e \approx \frac{\pi \sqrt{\pi}}{1.5u_e^3 k_D}, \quad (37a)$$

$$C_2^i \approx \frac{\pi \sqrt{\pi}}{2.9u_i^3 k_D}, \quad (37b)$$

$$S_2^\sigma \approx \frac{\pi \sqrt{\pi}}{2u_\sigma k_D}, \quad (37c)$$

which, aside from the difference in numerical factors, leads to a large-velocity dependence that is identical to that found in three dimensions [Eqs. (26)]. This correspondence, however, is only true for equilibrium plasmas. For nonequilibrium plasmas, the weak dynamical shielding of nonthermal particles becomes important.

3. Intermediate velocities

The intermediate velocity regime corresponds to $u_i > 1$ but $u_e < 1$. The coefficients due to the ions ($\sigma = i$) are identical to those for large velocities [Eqs. (37)], because the integrands are again sharply peaked. This fact has an important consequence: the coefficients due to the ions have no structure at \bar{v}_e . More generally, it can be shown that the coefficients due to a slow species have no structure at the thermal velocity of faster moving species. The converse is not true. For the coefficients due to the electrons, the approximation for $\text{Im } \xi_M$ is still a function of θ ,

$$\xi_M^2(\theta) \approx \frac{k_D^2}{4} [Z'(u_i \cos \theta) - 2], \quad (38)$$

so that it must be retained in the angular integrations

$$C_2^e \approx -\frac{2\pi}{k_D} \int_0^\pi d\theta \frac{\cos^2 \theta (1 - u_e^2 \cos^2 \theta)}{\text{Im} \sqrt{Z'(u_i \cos \theta) - 2}}, \quad (39a)$$

$$S_2^e \approx -\frac{2\pi}{k_D} \int_0^\pi d\theta \frac{\sin^2 \theta (1 - u_e^2 \cos^2 \theta)}{\text{Im} \sqrt{Z'(u_i \cos \theta) - 2}}. \quad (39b)$$

Even when the large-argument approximation to the Z' function is used, these are complicated functions of both u_e and u_i , and the interplay between the thermal velocities creates structure in the electron coefficients between the two thermal velocities. This is exactly what is observed in Fig. 2.

The following results hold for plasmas in thermal equilibrium. At both small and large velocities the Fokker-Planck coefficients behave similarly in two and three dimensions (aside from numerical factors that are geometrical in nature). In two dimensions the coefficients due to the electrons exhibit a complicated structure above the ion thermal velocity. This interplay between the thermal velocity scales increases in complexity when a population of energetic electrons is added.

C. Enhanced large-velocity interaction in two dimensions

We now turn to the most striking two-dimensional effect: the enhanced large-velocity interaction. This enhancement appears when there is a small, superthermal electron component. If this component is treated as a separate species,

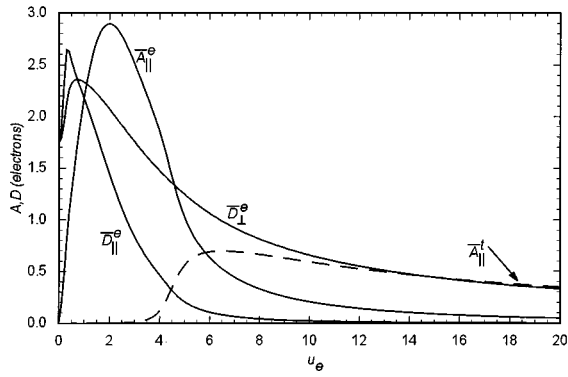


FIG. 3. Contribution of the bulk electrons to the Fokker–Planck coefficients of a test electron in a nonequilibrium two-dimensional plasma. The ion-to-electron mass ratio is 64, $n_i/n_e=0.01$, and $\bar{v}_i^2/\bar{v}_e^2=16$. The contribution of the tail electrons to the parallel drag, A_{\parallel}^t , is shown for comparison.

then the drag and diffusion due to these hot electrons are only weakly dependent on their density, i.e., even a small population of fast electrons can affect the transport significantly.

The choice of stable—but nonequilibrium—distribution is of three species: ions, bulk electrons, and tail electrons ($\sigma=i,e,t$), each with Maxwellian distributions characterized by thermal velocities \bar{v}_i , \bar{v}_e , and \bar{v}_t , respectively, where $\bar{v}_i < \bar{v}_e < \bar{v}_t$. Each component also has its own density (n_i, n_e, n_t) and hence its own plasma frequency (ω_{pi} , ω_{pe} , ω_{pt}). Figures 3 and 4 show the coefficients due to the bulk electrons and the tail electrons, respectively, for the parameters $\bar{v}_i^2/\bar{v}_e^2=16$ and $n_i/n_e=0.01$. Because the ions are the slowest species, the ion coefficients are unchanged from the equilibrium case, and are not shown. The coefficients due to the bulk electrons, as can be seen from Fig. 3, are also virtually unchanged from the equilibrium case, but they are shown for comparison with the coefficients due to the tail electrons.

The most striking aspect of Fig. 4 is the strength of the tail interaction at large velocities, $v > \bar{v}_t$. This strength is much larger than the density ratio would predict. The physical reason for this behavior is that because the wave emission

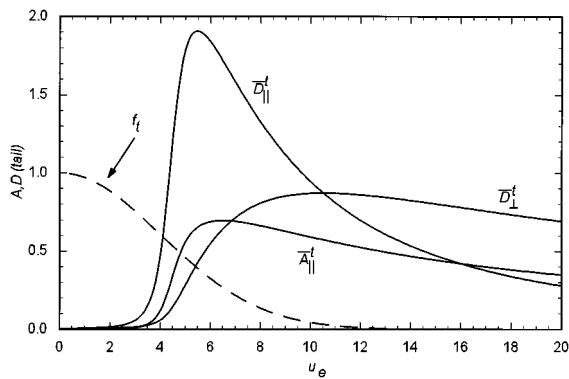


FIG. 4. Contribution of the tail electrons to the Fokker–Planck coefficients of a test electron in a nonequilibrium two-dimensional plasma. The ion-to-electron mass ratio is 64, $n_i/n_e=0.01$, and $\bar{v}_i^2/\bar{v}_e^2=16$. The distribution function of the tail electrons, f_t , is shown for comparison.

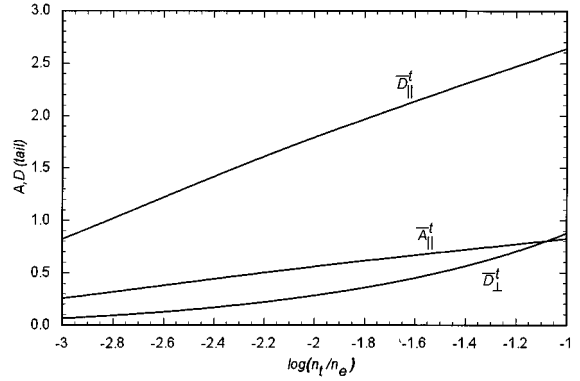


FIG. 5. Contribution of the tail electrons to the Fokker–Planck coefficients of a test electron in a nonequilibrium two-dimensional plasma, plotted as functions of the logarithm (base 10) of the tail density. The ion-to-electron mass ratio is 64, $u_e=5$, and $\bar{v}_i^2/\bar{v}_e^2=16$.

and the wave damping are both proportional to the density of the population, and because both are retained in the two-dimensional description, this density dependence cancels out for large velocities. To understand this behavior one must examine the large-velocity limits of C and S , where now the evaluation of $\xi_M(\theta_c)$ and $\xi_M(\theta_s)$ must take into account all three species.

As before, the evaluation of $\xi_M(\theta_c)$ depends on the species considered. For the tail electrons

$$\xi_M^2(\theta_c) \approx \frac{\omega_p^2}{2\bar{v}_t^2} - \frac{i}{2} \left(2\sqrt{\pi} \frac{\omega_{pe}^2 \bar{v}_t}{\bar{v}_e^2} e^{-\bar{v}_t^2/\bar{v}_e^2} + 1.3 \frac{\omega_{pt}^2}{\bar{v}_t^2} \right), \quad (40)$$

where $\omega_p^2 = \omega_{pi}^2 + \omega_{pe}^2$. The first term in the parentheses is the damping due to the bulk electrons, and the second is the damping due to the tail electrons. Equation (40) ignores the damping due to the ions as well as the correction to the dispersion relation due to the tail electrons. When $\bar{v}_t \gg \bar{v}_e$, the only significant damping arises from the tail electrons so that

$$\text{Im } \xi_M(\theta_c) \approx -0.46 \frac{\omega_{pt}^2}{\bar{v}_t \omega_p}, \quad (41)$$

which is proportional to the tail density. This implies

$$C_2^t \propto \frac{1}{n_t}. \quad (42)$$

Thus, both A_{\parallel}^t and D_{\parallel}^t are independent of n_t . Of course, this analysis only applies for large velocities. As v decreases, the damping due to the tail electrons increases more rapidly than the damping due to the bulk electrons (because $\bar{v}_t > \bar{v}_e$, and both are exponential). This continues until the damping due to the tail saturates near $v \approx \bar{v}_t$. In this region, the damping due to the bulk electrons becomes appreciable, and the largest term in $\text{Im } \xi_M^2(\theta_c)$ becomes the electron damping term, which is ignored in Eq. (41). For $v \approx \bar{v}_e$, the bulk damping dominates the tail damping and the coefficients due to the tail electrons revert to scaling linearly with density.

The density dependence of the coefficients due to the tail electrons is shown in Fig. 5. This figure shows the strength of the coefficients for $u_e=5$ as a function of the tail density,

n_t . It can be seen that on a logarithmic scale, A_{\parallel}^t and D_{\parallel}^t vary only linearly, while D_{\perp}^t exhibits a modicum of exponential behavior, which implies a stronger density dependence. To understand the behavior of D_{\perp}^t , S_2^t must be evaluated. The leading approximation, used in the case of thermal equilibrium, is to evaluate $\text{Im } \xi_M$ at $\theta = \theta_s$, which gives $\text{Im } \xi_M(\theta_s) \approx -k_D$. This leads to the expectation that D_{\perp}^t has the usual linear dependence on n_t , but in Fig. 5, D_{\perp}^t is not exponential, so it appears that there is some density independence. This arises because the width of the exponential in S is $1/u_t$, so that some of the behavior elucidated for C_2^t is included. It is a higher-order effect, however, and implies that D_{\perp}^t is more strongly density dependent than A_{\parallel}^t or D_{\parallel}^t , but is not proportional to n_t .

IV. COMPARISON WITH THREE DIMENSIONS

Recent work on diffusion in a strongly magnetized, three-dimensional plasma is closely related to the results presented in the previous section. Ware¹ derives a Fokker-Planck equation for the parallel distribution function of fast electrons in a three-dimensional, strongly magnetized plasma ($\omega_{ce} \gg \omega_{pe}$) due to wave emission and damping. He considers only the higher-order terms usually ignored by the dominant approximation in three dimensions, but that are similar in character to the lowest-order term that appears in two dimensions. Although he considers the case of a sheared magnetic field and a spatially nonuniform distribution function, the uniform limit of his result can be written as

$$\frac{\delta f}{\delta t} = -\frac{\partial}{\partial v_{\parallel}} (A_{\parallel} f) + \frac{1}{2} \frac{\partial}{\partial v_{\parallel}} \left(D_{\parallel} \frac{\partial f}{\partial v_{\parallel}} \right), \quad (43a)$$

$$A_{\parallel} = -\frac{2\pi n e^4}{m^2 v_{\parallel}^2}, \quad (43b)$$

$$D_{\parallel} = -\frac{2\pi n e^4}{m^2 v_{\parallel}^2} \left(\frac{F(v_{\parallel})}{\partial F(v_{\parallel}) / \partial v_{\parallel}} \right), \quad (43c)$$

where

$$F(v_{\parallel}) = \int d^2 v_{\perp} f(v_{\parallel}, v_{\perp}) \quad (44)$$

is the parallel electron distribution function. Here, the symbols \perp and \parallel refer to the direction of the magnetic field. Equations (43) are only applicable to test electrons with large velocities. While the drag A_{\parallel} is simply the large-velocity limit of the usual drag, the diffusion coefficient D_{\parallel} exhibits the behavior obtained for the two-dimensional problem. The denominator of Eq. (43c) is essentially the parallel Landau damping due to the total electron distribution function F and is analogous to the $\text{Im } \xi$ factor found in two dimensions. If F is expressed as the sum of two Maxwellians, one for the bulk electrons and one for the tail electrons (using our previous notation),

$$F = F_e + F_t = (1 - \eta_t) \frac{e^{-v_{\parallel}^2/2\bar{v}_e^2}}{\sqrt{2\pi}\bar{v}_e} + \eta_t \frac{e^{-v_{\parallel}^2/2\bar{v}_t^2}}{\sqrt{2\pi}\bar{v}_t}, \quad (45)$$

where η_t is that fraction of electrons that are in the tail, the derivative of F is

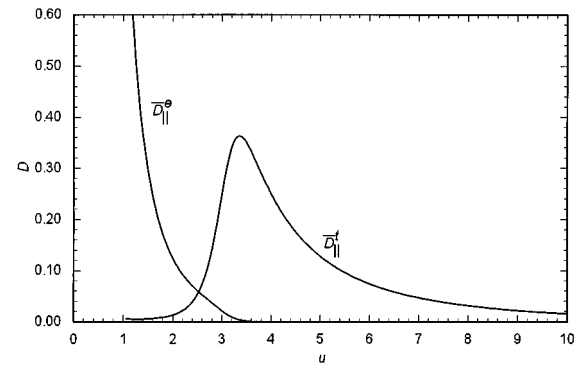


FIG. 6. Contribution of the electrons (both bulk and tail) to the parallel diffusion coefficient of a test electron in a nonequilibrium three-dimensional magnetized plasma, given by Eq. (47), with $\bar{v}_t^2/\bar{v}_e^2 = 16$ and $n_t/n_e = 0.01$. Compare with the two-dimensional equivalent in Figs. 3 and 4.

$$\frac{\partial F}{\partial v_{\parallel}} = -v_{\parallel} \left((1 - \eta_t) \frac{e^{-v_{\parallel}^2/2\bar{v}_e^2}}{\sqrt{2\pi}\bar{v}_e^3} + \eta_t \frac{e^{-v_{\parallel}^2/2\bar{v}_t^2}}{\sqrt{2\pi}\bar{v}_t^3} \right). \quad (46)$$

The two terms in the square brackets of Eq. (46) represent the damping due to the bulk electrons and the damping due to the tail electrons, respectively, similar in character to the imaginary part of Eq. (40). For those velocities such that the second term in the square brackets of Eq. (46) dominates the first, D_{\parallel} is independent of η_t . In order to compare with the two-dimensional results, D_{\parallel} is expressed as the sum of two terms, the diffusion due to the bulk electrons and the tail electrons,

$$D_{\parallel v} = \left(\frac{\sqrt{2}\pi n e^4}{m^2 \bar{v}_e} \right) (\bar{D}_{\parallel}^e + \bar{D}_{\parallel}^t). \quad (47)$$

The dimensionless diffusion coefficients obtained in this manner are shown in Fig. 6, for the same parameters used in Figs. 3 and 4, $\bar{v}_t^2/\bar{v}_e^2 = 16$ and $n_t/n_e = 0.01$. The enhanced large-velocity interaction is independent of the tail density, as can be seen from an expansion of \bar{D}_{\parallel}^t for large velocities,

$$\bar{D}_{\parallel}^t \approx 2\sqrt{2} \left(\frac{\bar{v}_t^2 \bar{v}_e}{v_{\parallel}^3} \right). \quad (48)$$

This is exactly the same behavior as in two dimensions, which shows that the enhanced interaction is due to the wave-driven transport, rather than an anomaly of the choice of only two dimensions.

The three-dimensional correction term³ in Eq. (20) has a form similar to the total integral in two dimensions: it is proportional to $(\text{Im } \xi)^{-1}$. All of the properties elucidated for two dimensions are therefore properties of the higher-order term that exists in three dimensions. In addition, Tidman and Eviatar³ showed that for large test-particle velocities (i.e., $v > \bar{v}_e$), the correction could be further approximated as

$$\frac{\pi \text{Re } \xi}{2 |\text{Im } \xi|} \approx \frac{1}{2v^2 |\partial F(v)/\partial v|}, \quad (49)$$

which is exactly equivalent in form (Landau damping in the denominator) to Eq. (43c), the three-dimensional strongly magnetized result. They also showed that for fast electrons,

the 90° deflection time is much shorter than the energy loss time, which means that the enhanced fluctuations scatter the fast electrons more quickly than they equilibrate with the bulk electrons. Because this process is the dominant one in two dimensions, this is the probable explanation for the two-dimensional particle simulation results of Decyk *et al.*⁸

Li and Petrasso²³ looked at higher-order terms in the context of three-dimensional binary collisions, but because they included only static shielding, their results do not contain the anomalous behavior.

V. FLUCTUATION SPECTRUM

Fast electrons, due to their undamped wave emissions, contribute significantly to the spectrum of fluctuations in a plasma.⁴ It is therefore instructive to consider the fluctuations in a two-dimensional plasma with fast electrons, and to investigate the connection between the form of the spectrum and the velocity-space transport coefficients. In the Appendix, the fluctuation spectrum $\mathcal{S}(\mathbf{k}, \omega)$ for arbitrary dimension is derived in the same manner as the Fokker–Planck coefficients. The result is

$$\mathcal{S}(\mathbf{k}, \omega) = (32\pi^3) \frac{\sum_{\sigma} n_{\sigma} q_{\sigma}^2 f_{\sigma}^1(\omega/k)}{k^3 |\epsilon(\mathbf{k}, \omega)|^2}, \quad (50)$$

which was first obtained by Hubbard.²⁴ If each species has a Maxwellian distribution with a common temperature, $T_{\sigma} = T$, this spectrum reduces to

$$\mathcal{S}(\mathbf{k}, \omega) \rightarrow \frac{8\pi T}{\omega} \text{Im} \frac{1}{\epsilon(\mathbf{k}, \omega)}, \quad (51)$$

which is simply a statement of the fluctuation–dissipation theorem. The fluctuation spectrum can be written in terms of $\text{Im} \epsilon^{-1}$ even when the plasma is not in equilibrium,

$$\mathcal{S}(\mathbf{k}, \omega) = \left(\frac{32\pi^2}{k} \right) \times \left(\frac{\sum_{\sigma} n_{\sigma} q_{\sigma}^2 f_{\sigma}^1(\omega/k)}{\sum_{\sigma} \omega_{p\sigma}^2 [\partial f_{\sigma}^1(v)/\partial v]_{v=\omega/k}} \right) \text{Im} \frac{1}{\epsilon(\mathbf{k}, \omega)}, \quad (52)$$

and this form shows the Landau damping expression in the denominator as before. It is well known that the diffusion coefficient can be written in terms of the fluctuation spectrum,

$$D = \frac{q^2}{m^2} \int \frac{d^3k}{(2\pi)^3} \frac{d\omega}{\nu} \mathbf{k} \mathbf{k} \mathcal{S}(\mathbf{k}, \omega) \delta(\omega - \mathbf{k} \cdot \mathbf{v}), \quad (53)$$

and the insertion of Eq. (52) into Eq. (53) results in a form for the diffusion coefficient very similar to that found by Ware.¹

The frequency spectrum $S(\omega)$ is defined as the integral over \mathbf{k} of $\mathcal{S}(\mathbf{k}, \omega)$, and can be expressed as a sum over species,

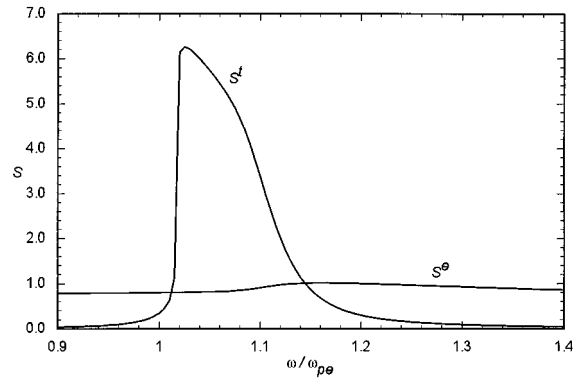


FIG. 7. Contribution of the electrons (both bulk and tail) to the two-dimensional frequency spectrum $S(\omega)$ for the same parameters as in Figs. 3 and 4, $n_i/n_e = 0.01$ and $\bar{v}_i^2/\bar{v}_e^2 = 16$.

$$S(\omega) \equiv \int \frac{d^3k}{(2\pi)^3} \mathcal{S}(\mathbf{k}, \omega), \quad (54a)$$

$$= \frac{4}{(2\pi)^{v-3}} \sum_{\sigma} n_{\sigma} q_{\sigma}^2 \int d^3k \frac{f_{\sigma}^1(\omega/k)}{k^3 |\epsilon(\mathbf{k}, \omega)|^2}, \quad (54b)$$

$$\equiv \sum_{\sigma} S^{\sigma}(\omega). \quad (54c)$$

Except for missing a factor of $k^2 q^2/m^2$, it is identical with D_{\parallel} when the substitution $\omega/k \rightarrow v \cos \theta$ is made. As a function of ω , $S(\omega)$ exhibits similar properties to $D_{\parallel}(v)$. The analysis, however, is complicated by the fact that the integrand over dk cannot be expressed as a simple pole, due to the complexity of the Z function. Nevertheless, for those regions in (\mathbf{k}, ω) space where the damping due to the tail electrons is larger than the damping due to the bulk electrons, the tail electrons make a density-independent contribution to the frequency spectrum. This behavior is clearly seen in Fig. 7, where the contributions to the frequency spectrum $S(\omega)$ due to the bulk electrons and the tail electrons are shown (for the same parameters as Figs. 3 and 4). As is well known, the frequency spectrum for a plasma in thermodynamic equilibrium has a small peak just above the plasma frequency, due to the electron plasma waves.²⁵ For a two-dimensional plasma with a hot electron component, this peak is enhanced, and the strength of the enhancement is due to the tail electrons and is relatively independent of their density.

Mace *et al.*²⁶ have investigated the fluctuation spectrum for three-dimensional, unmagnetized, isotropic plasmas whose velocity distribution is a so-called kappa distribution. Because these distributions have an excess of suprathermal particles, there is an enhanced level of fluctuations near the plasma frequency, in agreement with the present work. Also, a two-temperature electron distribution (due to photoelectrons) has been used to interpret spectral measurements in the magnetosphere.²⁷

VI. CONCLUSION

We have investigated an effect that is inherent to weakly stable plasmas: an enhanced large-velocity interaction. This

behavior is not unique to two dimensions, but is quite similar to the higher-order terms in a three-dimensional dominant approximation expansion, as shown in the studies of Ware¹ and of Tidman and Eviatar.³ The increased level of fluctuations generated by fast electrons is quite similar in both two and three dimensions. However, because both the emission and absorption of fluctuations by fast electrons is retained by the two-dimensional Fokker–Planck theory to lowest order (no dominant approximation is needed), these electrons interact at a significantly higher level than predicted by an extrapolation based on the usual three-dimensional dominant calculation. Small-angle collisions do not dominate in two dimensions, and the soft core of the logarithmic potential implies that any enhanced fluctuations affect the transport significantly. In three dimensions, a substantial tail would be necessary before a corresponding effect is observed.^{4,5} These results are essential to a complete understanding of two-dimensional particle simulations, especially those of weakly stable plasmas.

ACKNOWLEDGMENT

This work is sponsored by the Office of Naval Research.

APPENDIX: CALCULATION OF FLUCTUATIONS

In order to calculate the fluctuation integral properly in fewer than three dimensions, some care is needed in implementing the ensemble average and performing the Fourier transforms. The specific treatment is due to Fried,²⁸ although it is formally equivalent to the method of Lenard.¹⁴ The starting point is the Klimontovich–Poisson system of equations (i.e., electrostatic) for an unmagnetized plasma, which determine the exact, microscopic distribution function \tilde{f} and the exact, microscopic electric field $\tilde{\mathbf{E}}$,

$$\left(\frac{\partial}{\partial t} + \mathbf{v} \cdot \nabla + \frac{q}{m} \tilde{\mathbf{E}} \cdot \frac{\partial}{\partial \mathbf{v}} \right) \tilde{f} = 0, \quad (\text{A1a})$$

$$\nabla \cdot \tilde{\mathbf{E}} = 4\pi \sum_{\sigma} n_{\sigma} q_{\sigma} \int d^{\nu} v \tilde{f}. \quad (\text{A1b})$$

The ensemble average of an exact quantity \tilde{A} is defined as $A \equiv \langle \tilde{A} \rangle$, so that the fluctuation from the ensemble average is $\delta A \equiv \tilde{A} - A$. The ensemble average of \tilde{f} is the usual one-body distribution function $f = \langle \tilde{f} \rangle$. The ensemble average of Eqs. (A1) results in two systems of equations: those that govern the average quantities (f and \mathbf{E}) and those that govern the fluctuations (δf and $\delta \mathbf{E}$). The quasilinear approximation (not to be confused with Quasilinear Theory²⁹) consists of ignoring the higher-order terms when solving for the fluctuations, and assuming that δf and $\delta \mathbf{E}$ evolve on much faster temporal and spatial scales than f and \mathbf{E} . The fluctuations drive changes in the average quantities, and the fluctuation integral can be written as

$$\frac{\delta f}{\delta t} = -\frac{q}{m} \frac{\partial}{\partial \mathbf{v}} \cdot \langle \delta \mathbf{E} \delta f \rangle. \quad (\text{A2})$$

Under this approximation, the equations for the fluctuations are identical to the linearized Vlasov–Poisson system, where δf and $\delta \mathbf{E}$ are the first-order quantities and f is the zeroth-order distribution function

$$\left(\frac{\partial}{\partial t} + \mathbf{v} \cdot \nabla + \frac{q}{m} \mathbf{E} \cdot \frac{\partial}{\partial \mathbf{v}} \right) \delta f(\mathbf{x}, \mathbf{v}, t) = -\frac{q}{m} \delta \mathbf{E}(\mathbf{x}, t) \cdot \frac{\partial}{\partial \mathbf{v}} f(\mathbf{v}), \quad (\text{A3a})$$

$$\nabla \cdot \delta \mathbf{E}(\mathbf{x}, t) = 4\pi \sum_{\sigma} n_{\sigma} q_{\sigma} \int d^{\nu} v \delta f(\mathbf{x}, \mathbf{v}, t). \quad (\text{A3b})$$

The distribution f is not a function of \mathbf{x} or t because it is assumed to be uniform on the scale over which δf evolves. The solution to Eqs. (A3) is well known, and is found by Fourier–Laplace transforming, i.e., in the context of an initial-value problem. The solution is algebraic and both δf and $\delta \mathbf{E}$ are proportional to the initial fluctuations in the system $\delta f(\mathbf{k}, \mathbf{v}, t=0)$. Transforming back to time and taking the long time limit, $t \rightarrow \infty$, it is found that the fluctuations are driven only by the free-streaming terms ($\mathbf{k} \cdot \mathbf{v} = \omega$) as long as the plasma is stable ($\text{Im } \omega < 0$ for $\epsilon = 0$). Finally, the spatial Fourier transforms must be inverted to evaluate the quantity $\langle \delta \mathbf{E} \delta f \rangle$. The ensemble average of the initial fluctuations is

$$\begin{aligned} & \langle \delta f_{\sigma}^*(\mathbf{k}, \mathbf{v}_{\sigma}, 0) \delta f_{\alpha}(\mathbf{k}', \mathbf{v}_{\alpha}, 0) \rangle \\ &= \frac{(2\pi)^{\nu}}{n_{\sigma}} f_{\sigma}(\mathbf{v}_{\sigma}) \delta(\mathbf{k} - \mathbf{k}') \delta(\mathbf{v}_{\sigma} - \mathbf{v}_{\alpha}) \delta_{\sigma\alpha}, \end{aligned} \quad (\text{A4})$$

where the factor of $(2\pi)^{\nu}$ comes from collapsing the inverse transform. The only dependence on ν is the exponent of 2π , and the answer is

$$\frac{\delta f}{\delta t} = -\frac{\partial}{\partial \mathbf{v}} \cdot \mathbf{J}(\mathbf{v}), \quad (\text{A5a})$$

$$\begin{aligned} \mathbf{J}(\mathbf{v}) = & \frac{1}{(2\pi)^{\nu-3}} \sum_{\sigma} \int d^{\nu} v_{\sigma} \left(\frac{f(\mathbf{v})}{m_{\sigma}} \frac{\partial f_{\sigma}(\mathbf{v}_{\sigma})}{\partial \mathbf{v}_{\sigma}} \right. \\ & \left. - \frac{f_{\sigma}(\mathbf{v}_{\sigma})}{m} \frac{\partial f(\mathbf{v})}{\partial \mathbf{v}} \right) \cdot \mathbf{K}, \end{aligned} \quad (\text{A5b})$$

$$\mathbf{K} = \frac{2q^2 q_{\sigma}^2 n_{\sigma}}{m} \int d^{\nu} k \frac{\delta(\mathbf{k} \cdot \mathbf{v} - \mathbf{k} \cdot \mathbf{v}_{\sigma})}{|\epsilon(\mathbf{k}, \mathbf{k} \cdot \mathbf{v})|^2} \frac{\mathbf{k} \mathbf{k}}{k^4}. \quad (\text{A5c})$$

This formalism allows the calculation of another quantity of interest, the fluctuation spectrum $\mathcal{S}(\mathbf{k}, \omega)$, which is defined as the transform of the fluctuating electric field squared,

$$\langle \delta E(\mathbf{x}, t) \delta E(\mathbf{x}, t) \rangle \equiv \int \frac{d^{\nu} k d\omega}{(2\pi)^{\nu+1}} \mathcal{S}(\mathbf{k}, \omega). \quad (\text{A6})$$

The evaluation of $\langle \delta E \delta E \rangle$ proceeds in the same manner as the evaluation of $\langle \delta \mathbf{E} \delta f \rangle$ above. The inverse transforms are evaluated with the help of Eq. (A4), and the spectrum is²⁴

$$\mathcal{S}(\mathbf{k}, \omega) = (32\pi^3) \frac{\sum_{\sigma} n_{\sigma} q_{\sigma}^2 f_{\sigma}^1(\omega/k)}{k^3 |\epsilon(\mathbf{k}, \omega)|^2}. \quad (\text{A7})$$

The same result is obtained if one calculates the electric field due to a test particle δE , and then integrates the result over all the plasma particles.

- ¹A. A. Ware, Phys. Fluids B **5**, 2769 (1993).
- ²S. Chandrasekhar, Rev. Mod. Phys. **15**, 1 (1943).
- ³D. A. Tidman and A. Eviatar, Phys. Fluids **8**, 2059 (1965).
- ⁴F. Perkins and E. E. Salpeter, Phys. Rev. **139**, A55 (1965).
- ⁵G. Joyce, D. Montgomery, and C. Roqué, Phys. Fluids **10**, 2399 (1967).
- ⁶H. Okuda and C. K. Birdsall, Phys. Fluids **13**, 2123 (1970).
- ⁷A. B. Langdon and C. K. Birdsall, Phys. Fluids **13**, 2115 (1970).
- ⁸V. K. Decyk, G. J. Morales, J. M. Dawson, and H. Abe, in *13th European Conference on Controlled Fusion and Plasma Heating*, Schliersee, 1986, edited by G. Brifford and M. Kaufman (European Physical Society, Petit-Lancy, 1986), p. 358.
- ⁹L. D. Landau, Zh. Eksp. Teor. Fiz. **7**, 203 (1937), reprinted in *Collected Papers of L. D. Landau*, edited by D. ter Haar (Pergamon, New York, 1965), p. 163.
- ¹⁰R. S. Cohen, L. Spitzer, Jr., and P. McR. Routly, Phys. Rev. **80**, 230 (1950).
- ¹¹M. N. Rosenbluth, W. M. MacDonald, and D. L. Judd, Phys. Rev. **107**, 1 (1957).
- ¹²M. A. Reynolds, Ph.D. dissertation, University of California, Los Angeles, 1995.
- ¹³C. D. Decker, W. B. Mori, J. M. Dawson, and T. Katsouleas, Phys. Plasmas **1**, 4043 (1994).
- ¹⁴A. Lenard, Ann. Phys. (N.Y.) **3**, 390 (1960).
- ¹⁵B. D. Fried and S. D. Conte, *The Plasma Dispersion Function* (Academic, New York, 1961).
- ¹⁶B. Abraham-Shrauner, Physica **43**, 95 (1969).
- ¹⁷J. Dawson, Phys. Fluids **5**, 45 (1962).
- ¹⁸J. M. Dawson, Phys. Fluids **7**, 419 (1964).
- ¹⁹O. C. Eldridge and M. Feix, Phys. Fluids **5**, 1076 (1962).
- ²⁰O. C. Eldridge and M. Feix, Phys. Fluids **5**, 1307 (1962).
- ²¹J. L. Rouet and M. R. Feix, Phys. Plasmas **3**, 2538 (1996).
- ²²S. Ichimaru, *Basic Principles of Plasma Physics: A Statistical Approach* (Benjamin, Reading, MA, 1973), Chap. 10.
- ²³C.-K. Li and R. D. Petrasso, Phys. Rev. Lett. **70**, 3063 (1993).
- ²⁴J. Hubbard, Proc. R Soc. London, Ser. A **260**, 114 (1961).
- ²⁵J. M. Dawson and C. Oberman, Phys. Fluids **5**, 517 (1962).
- ²⁶R. L. Mace, M. A. Hellberg, and R. A. Treumann, "Electrostatic fluctuations in plasmas containing suprathermal particles," submitted to J. Plasma Phys.
- ²⁷E. J. Lund, J. LaBelle, and R. A. Treumann, J. Geophys. Res. **99**, 23 651 (1994).
- ²⁸B. D. Fried, in *Plasma Physics in Theory and Application*, edited by W. B. Kunkel (McGraw-Hill, New York, 1966), Chap. 3.
- ²⁹A. A. Vedenov, E. P. Velikhov, and R. Z. Sagdeev, Nucl. Fusion **1**, 82 (1961); W. E. Drummond and D. Pines, Nucl. Fusion Suppl. **3**, 1049 (1962).